A MULTIPOLE EXPANSION FOR THE FIELD OF VACUUM CHAMBER EDDY CURRENTS*

S.Y. Lee

Brookhaven National Laboratory
Upton, NY 11973 USA

Abstract

Analytic formula for the multipole coefficients of a single current filament between two infinitely-permeable iron plates are obtained. These are applied to the eddy currents generated in a two-dimensional conducting surface, such as a synchrotron vacuum chamber, when it is exposed to a rapidly varying magnetic field. We find that the sextupole component, b_2, is insensitive to the chamber shape and depends only on the gap between the plates, if the width of the chamber is much larger than the height. Higher multipoles, b_n decrease rapidly with increasing chamber width. The radius of convergence for the multipole expansion, at least up to $n = 10$, is about 80% of the width of the chamber.

1. Introduction

A rapid cycling synchrotron may have $\dot{B}/B \geq 25$ sec^{-1}, with resulting large eddy currents in conductors in the field. In some electron machines, it has been necessary to make the beam vacuum chamber of a non-conductor to eliminate time-dependent field perturbations, but such chambers are difficult to make. In the absence of iron, two chamber shapes, circular and rectangular geometries, have simple analytical solutions. The eddy currents in a circular chamber in the uniform field generate a pure dipole field in its interior, and eddy currents in a rectangular vacuum chamber generate dominantly a sextupole superimposed on a dipole field.[1] When the chamber is between iron poles, which can be approximated by infinite permeability upper and lower plane boundaries, the solutions are not so simple and numerical solutions are frequently resorted to.[1] It is therefore useful to extend analytic calculations of harmonic content to this situation, at least in the case of several common chamber geometries, e.g., rectangular, circular and elliptical.

In Section 2 we compute expansion coefficients analytically, in Section 3 the multipole coefficients are compared with numerical calculations, and conclusions are given in Section 4.

2. Analytical Calculation of Harmonics

A) The Field of a Single Filament

Using Beth's[3] complex representation for the field $H = H_y + iH_x$, it is shown in the Appendix that the field at z of a current filament at $z_c = x_c + iy_c$, both points between parallel, infinite permeability plates, is given by

$$H = \frac{I}{4\,g}\left(\tanh\frac{\pi\,(z-z_c^*)}{2\,g} + \coth\frac{\pi\,(z-z_c)}{2\,g}\right), \qquad (1)$$

where I is the current and g is the gap between the iron plates. The field can be expanded in a Taylor series about the origin,

$$\begin{aligned} B &= \frac{\mu_0 I}{4g}\sum_{n=0}^{\infty}\frac{1}{n!}\left(\alpha_n+\beta_n\right)\left(\frac{\pi}{2g}\right)^n z^n \\ &= \sum_{n=0}^{\infty}\left(B_n + iA_n\right) z^n \end{aligned} \qquad (2)$$

where

$$\alpha_n = \left.\frac{\partial^n \tanh\left(z-\frac{\pi z_c^*}{2g}\right)}{\partial z^n}\right|_{z=0} \qquad (3)$$

and

$$\beta_n = \left.\frac{\partial^n \coth\left(z-\frac{\pi z_c}{2g}\right)}{\partial z^n}\right|_{z=0} \qquad (4)$$

are listed in Table 1.

Table 1: Multipole Coefficients of a Single Wire.

n	$\alpha_n \quad t \equiv \tanh\left(-\frac{\pi z_c^*}{2g}\right) \quad c \equiv \cosh\left(-\frac{\pi z_c^*}{2g}\right)$
0	t
1	c^{-2}
2	$-2tc^{-2}$
3	$-2c^{-4} + 4t^2c^{-2}$
4	$16tc^{-4} - 8t^3c^{-2}$
5	$16c^{-6} - 88t^2c^{-4} + 16t^4c^{-2}$
6	$-272tc^{-6} + 416t^3c^{-4} - 32t^5c^{-2}$
7	$-272c^{-8} + 2880t^2c^{-6} - 1824t^4c^{-4} + 64t^6c^{-2}$
8	$7936tc^{-8} - 24576t^3c^{-6} + 7680t^5c^{-4} - 128t^7c^{-2}$
n	$\beta_n \quad \tilde{t} \equiv \coth\left(-\frac{\pi z_c}{2g}\right) \quad s \equiv \sinh\left(-\frac{\pi z_c}{2g}\right)$
0	$\tilde{t}$
1	$-s^{-2}$
2	$2\tilde{t}s^{-2}$
3	$-2s^{-4} - 4\tilde{t}^2s^{-2}$
4	$16\tilde{t}s^{-4} + 8\tilde{t}^3s^{-2}$
5	$-16s^{-6} - 88\tilde{t}^2s^{-4} - 16\tilde{t}^4s^{-2}$
6	$272\tilde{t}s^{-6} + 416\tilde{t}^3s^{-4} + 32\tilde{t}^5s^{-2}$
7	$-272s^{-8} - 2880\tilde{t}^2s^{-6} - 1824\tilde{t}^4s^{-4} - 64\tilde{t}^6s^{-2}$
8	$7936\tilde{t}s^{-8} + 24576\tilde{t}^3s^{-6} + 7680\tilde{t}^5s^{-4} + 128\tilde{t}^7s^{-2}$

Note that when $|\frac{\pi z_c}{2g}| >> 1$, we have

$$\begin{aligned} \tanh\left(-\frac{\pi z_c^*}{2g}\right) &\longrightarrow \pm 1 \\ \coth\left(-\frac{\pi z_c}{2g}\right) &\longrightarrow \pm 1 \\ \sinh\left(-\frac{\pi z_c}{2g}\right) &\sim \pm\frac{1}{2}e^{|\frac{\pi x_c}{2g}|\pm i\frac{\pi y_c}{2g}} \\ \cosh\left(-\frac{\pi z_c^*}{2g}\right) &\sim \frac{1}{2}e^{|\frac{\pi x_c}{2g}|\pm i\frac{\pi y_c}{2g}} \end{aligned}$$

Thus the current filament far away from the origin, $x_c >> g$, produces mainly dipole field. On the other hand, the multipole component is most sensitive to those current filament located at $x_c < g$.

For a given distribution of current filament, the total magnetic field is then obtained from the line integral (or surface

* Work performed under the auspices of the U.S. Department of Energy.

integral for current density) along the source current filament, i.e.

$$B(z) = \frac{\mu_0}{4g} \int_{\text{source}} ds_c I(z_c) \left[\coth \frac{\pi (z - z_c^*)}{2g} + \tanh \frac{\pi (z - z_c)}{2g} \right] \tag{5}$$

Similarly, the multipole coefficients of Eq. (2) are obtained from the line (or surface) integral of these α, β's coefficients in Table 1, i.e.

$$B_n + iA_n = \frac{\mu_0}{2\pi n!} \int_{\text{source}} ds_c I(z_c)(\alpha_n + \beta_n) \left(\frac{\pi}{2g} \right)^{n+1} \tag{6}$$

3. The Field due to Eddy Currents in a Vacuum Chamber Wall

If the main dipole field B is uniform, and there is no net transport current, the induced current density $j = \sigma \dot{B} x$, where σ is the electrical resistivity, $\dot{B}$ is the rate of change of field and x is distance measured from the chamber center. The chamber wall is assumed to be symmetric about the horizontal and vertical axes and of uniform thickness h. We consider the basic shapes of a circle, ellipse and rectangle, with a and b denoting the half width and half height, respectively. For example, the elliptical chamber is described by

$$x^2/a^2 + y^2/b^2 = 1 \tag{7}$$

and the rectangular chamber by

$$x = \pm a \text{ for } y \in (-b, b) \text{ and } y = \pm b \text{ for } x \in (-a, a) \tag{8}$$

The multipole coefficients of Eq. (6) are obtained by integrating over the chamber wall, thus:

$$b_n + ia_n = \frac{\mu_0 \sigma h \dot{B}}{2\pi n! B} \left(\frac{\pi}{2g} \right)^{n+1} \int_{v.c.} x(\alpha_n + \beta_n) ds \tag{9}$$

where α_n and β_n are given by Table 1 and

$$b_n + ia_n \equiv (B_n + iA_n)/B \ .$$

When the vacuum chamber is symmetric with respect to the horizontal mid-plane, the integral in Eq. (9) becomes real, i.e. the skew multipole coefficients a_n are zero. Similarly when the vacuum chamber is symmetric with respect to vertical mid-plane, multipoles with n =odd vanish. Most of the vacuum chamber satisfies the above symmetries, we expect therefore only n = even multipoles.

Equation (9) has also interesting scaling property, i.e. when the vacuum chamber size increases (or decreases) proportional to the gap, g, the multipole coefficient would also scale as

$$b_n \propto g^{-n+1}$$

However, when g is constant while the vacuum chamber size is changed, the scaling property is much more complicated. We tabulate the multipole coefficients for the following possible parameters of fast cycling synchrotron,

$$\begin{aligned} h &= 1mm \\ \sigma^{-1} &= 0.8\mu\Omega m \\ \dot{B}/B &= 30/sec \\ g &= 5.715cm \\ b &= 2cm \end{aligned}$$

for various vacuum chamber half width a. Note that b_2 increases toward a limiting value of $b_2 = 0.824$ m^{-2} by the following equation:[1]

$$b_2 \simeq \frac{\mu_o \sigma h \dot{B}}{Bg} \tag{11}$$

which can be obtained from Eq. (9) in the limit of $a/g >> 1$.

It is interesting to observe that the multipole coefficients ($n > 2$) for the circular vacuum chamber, shown in the first column of Table 2, is not small due to the image current. The higher multipoles b_n ($n > 12$) scales *well* with a^{-n}, i.e.

$$b_n \simeq 0.01 \frac{\mu_0 \sigma h \dot{B}}{B} \cdot b\, a^{-n} \quad (n \geq 12) \tag{12}$$

Thus the higher multipole coefficients become smaller for a larger width of vacuum chamber. For a fixed b/a, ratio between the semi-minor axis to the semi-major axis, the multipole coefficients would scale with $a^{-(n-1)}$. The scaling property is thus similar to that of superconducting magnets. For intermediate multipole coefficients, $4 \leq n \leq 12$, $b_n \propto a^{-m}$ with $m < n$ and depends more sensitively on other geometric parameters. These multipole coefficients decreased as the width of the vacuum chamber is increased. The multipole coefficients is in general small when the eccentricity ratio $b/a \leq \frac{1}{2}$. For the rectangular vacuum chamber, the scaling is obscured by the sign variation with respect to the width parameter a. The multipole coefficients is in general small at small b/a ratio. The sextupole and dipole components are larger than that of elliptical geometry.

Table 2: b_n Coefficients [m^{-n}] for Elliptical Vacuum Chamber

a[cm]	2	4	6
b_0 [$\times 10^{-3}$]	-0.634	-1.69	-3.39
b_2	0.160	0.502	0.670
b_4 [$\times 10$]	6.80	-5.09	-2.93
b_6 [$\times 10^3$]	327.	16.3	0.911
b_8 [$\times 10^6$]	747.	3.41	0.665
b_{10} [$\times 10^8$]	18837.	16.9	0.681
b_{12} [$\times 10^{10}$]	233348.	61.5	0.312

3.1 Radius of Convergence for the Multipole Expansion

Since the magnetic field due to the current filament has a simple pole at the source location, the radius of convergence r for the expansion would be equal to the radius of the filament R_c. As $r \to R_c$, the number of terms needed in the multipole expansion becomes large. In most of numerical calculation by using PE2D program, the accuracy is limited to multipoles $n \leq 10$. We thus study the radius of convergence for multipole expansion up to $n \leq 10$ even when the higher multipoles $N > 10$ can be calculated accurately in the present method.

Beyond the radius of convergence, the exact field obtained from Eq. (5) would deviate from Eq. (2) of multipole expansion with little improvement by including higher multipoles ($n > 10$). Figure 1 shows an example of comparison between exact and multipole expansion along the horizontal axis. For a single coil, it is in general about 80% of the coil radius For a special designed current distribution, such as $\cos\theta$ in the superconducting magnet or the conventional H-magnet, the radius of convergence equal to the coil radius (in fact, these special magnets have ideally only b_0 term).

4. Conclusion

We have obtained an analytic formula for the magnetic field and the multipole coefficients of a single filament between two infinitely permeable iron plates. The method is then applied to the eddy currents generated in a two dimensional conducting tube, such as a synchrotron vacuum chamber exposed to a rapidly varying magnetic field. The analytic method is then compared with the numerical method of PE2D. We found that the eddy

current multipole is sensitive to the vacuum chamber geometry. Elliptical vacuum chamber geometry with eccentricity parameter $b/a \leq \frac{1}{2}$ gives in general small higher multipolar strength. On the other hand, the higher multipole coefficients are larger for diamond or polygon shape vacuum chambers. The effect of the eddy current multipoles ($n \geq 4$) on the beam dynamics is small provided that the beam size is less than 50% of vacuum chamber width. On the other hand, when the beam size is expected to be 2/3 of the vacuum chamber width, the shape of vacuum chamber may be important, where the elliptical vacuum chamber gives small multipole strengths.

References

1. D.A. Edward and M.J. Syphers, AIP Conf. Proc. 184, ed. M. Month and M. Dienes, p. 79 (1988).
2. G. Morgan and S. Kahn, AGS Booster Technical Note No. 4.
3. R.A. Beth, "Complex Representation and Computation of two dimensional magnetic fields", J. App. Phys, **37**, 2568 (1966).

Appendix A. Magnetic Field due to a Current Filament in the Parallel Plates with Infinite Permeability

The magnetic field $H = H_y + iH_x$ measured at a $z = x + iy$ due to an infinite long filament with current I located at $z_c = x_c + iy_c$ is given by[3]

$$H = \frac{I}{2\pi (z - z_c)} \tag{A.1}$$

When the current filament is located inside the two parallel iron plates with infinite permeability. The boundary condition for the field at the interface between the air and the iron plate can easily be achieved by using the image current method. Because of two parallel plates, the image currents of the source current I at z_c are located at

$$z_c^* \pm img \quad m = 1, 3, 5, \ldots$$
$$z_c \pm img \quad m = 2, 4, 6, \ldots$$

where g is the gap distance between these two iron plates. The magnetic field inside the parallel plates can be expressed in terms of the linear combination of these currents, i.e.

$$H = \frac{I}{2\pi (z - z_c)} + \frac{I}{2\pi} \sum_{m=1,3} \left[\frac{1}{(z - z_c^* + img)} + \frac{1}{(z - z_c^* - img)} \right] + \frac{I}{2\pi} \sum_{m=2,4,\ldots} \left[\frac{1}{(z - z_c + img)} + \frac{1}{(z - z_c - img)} \right] \tag{A.2}$$

The series can easily be summed to give

$$H = \frac{I}{4g} \left[\tanh \frac{\pi (z - z_c^*)}{2g} + \coth \frac{\pi (z - z_c)}{2g} \right] \tag{A.3}$$

Note the singularity of a simple pole at $z = z_c$ is retained in Eq. (A.3).

Appendix B. Power Loss on the Vacuum Chamber Wall

The power dissipated per unit length on the vacuum chamber wall due to the eddy current is given by

$$\frac{dp}{d\ell} = \sigma h \dot{B}^2 \int_{v.c.} x^2 ds \equiv \sigma h \dot{B}^2 a^3 G_p \tag{B.1}$$

where a is width of the vacuum chamber, G_p is the geometric factor. Some of the geometric factors are listed in the following:

(1) Rectangle

$$G_p = 4 \left(\frac{1}{3} + \epsilon \right)$$

(2) Polygon of Eq. (13)

$$G_p = 4 \left(1 + m^2\right)^{1/2} / 3 + \epsilon - m$$

(3) Ellipse

$$G_p = 4 \int_0^{\pi/2} \sin \varphi \left(\cos^2 \varphi + \epsilon^2 \sin^2 \varphi \right)^{1/2} d\varphi$$

where $\epsilon = b/a$.

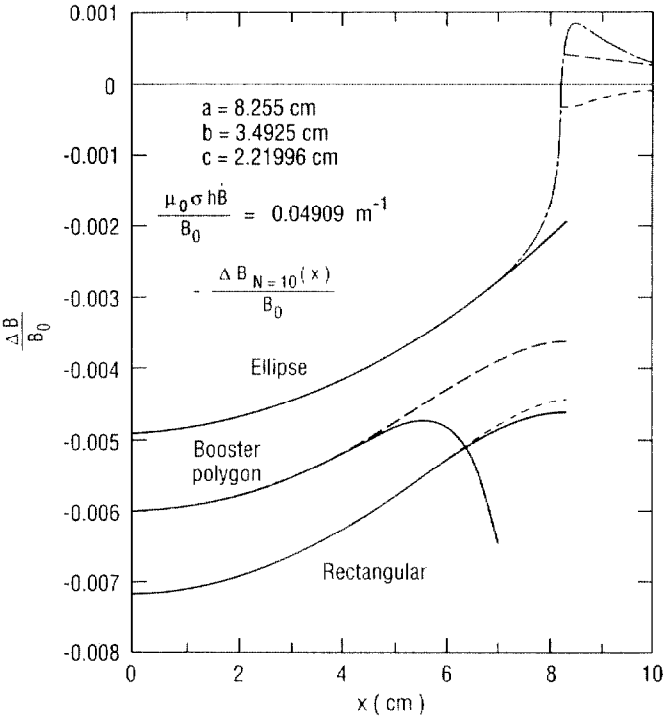

Figure 1: Comparison of eddy current field for three different shapes of vacuum chamber with same width and height. The solid line represents the multipole expansion up to $n = 10$ pole. The dashed curves represent the exact field. The multipole expansion diverges at $x > 5$ cm for the booster polygon shape.